Electronic Supporting Information

Ferroelectric and Field-Induced Ferroelectric Phase Formations in Atomic-Layer-Deposited ZrO_2 Thin Films with TiN Electrodes †

Jae Hee Song,[a,b] Kyung Do Kim,[a] Jonghoon Shin,[a] Seong Jae Shin,[a] Suk Hyun Lee,[a] Seung Yong Byun,[a] In Soo Lee,[a] Han Sol Park,[a] Yeon Jae Kim,[a,b] Hyun Woo Nam,[a,b] and Cheol Seong Hwang*[a]

a Department of Materials Science and Engineering, and Inter-University Semiconductor Research Center, Seoul National University, Seoul, 08826, Republic of Korea. E-mail: cheolsh@snu.ac.kr

b SK Hynix Semiconductor, Inc., Icheon, Gyeonggi 17336, Republic of Korea.

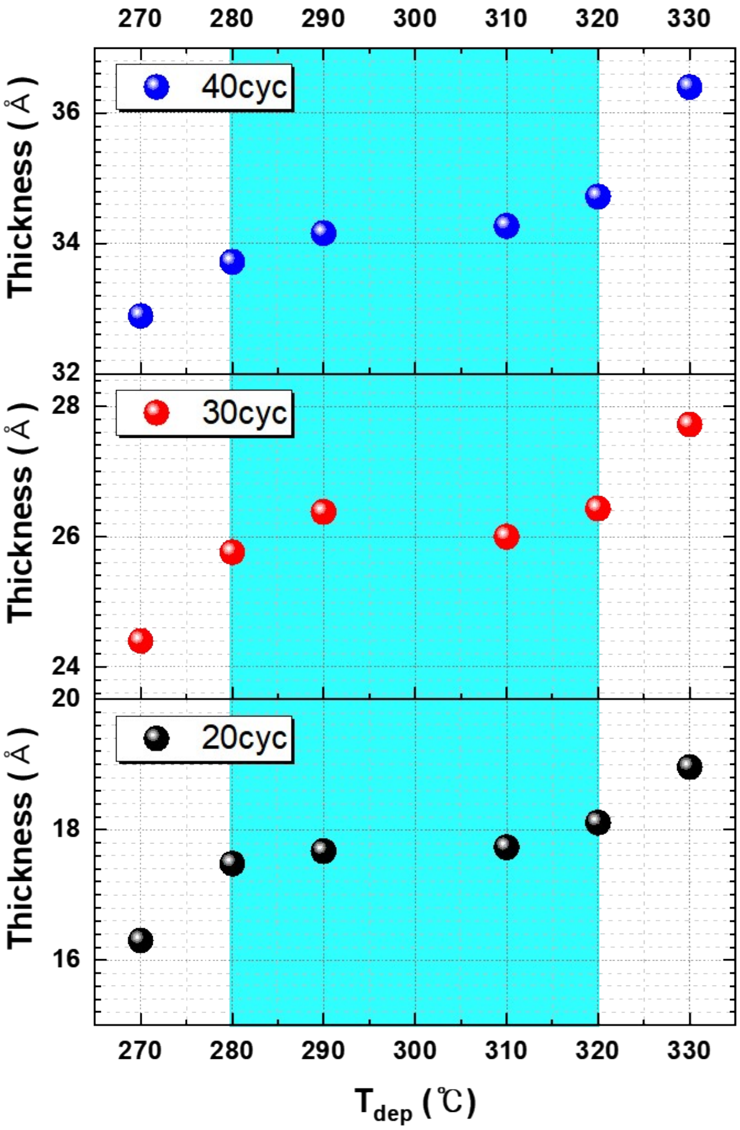

Figure S1. ALD ZrO_2 temperature window of the Si substrate. The thickness of ZrO_2 thin films according to cycle counts of 20 (black), 30 (red), and 40 (blue) is similar between T_{dep} of 280 and 320 °C.

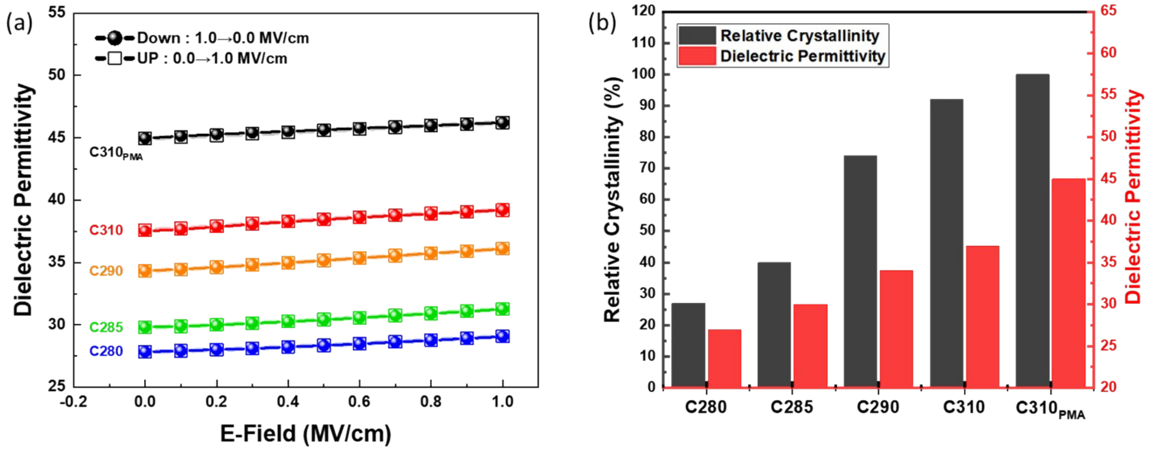

Figure S2. (a) Dielectric permittivity of pristine 10-nm-thick C280–C310 and C310$_{PMA}$ samples. Measurements were performed using a 10 kHz sweep in the 0–1.0 V range to exclude switching-related contributions. (b) Relative crystallinity and dielectric permittivity of the same samples. Crystallinity was calculated by extracting the main XRD peak area for each sample and normalizing it to the value of C310$_{PMA}$, which was set to 100.

Considering the reported dielectric constant of amorphous ZrO_2 (~22)[1], the dielectric permittivity of C280–C310 (ranging from ~27 to ~37) increases with crystallinity, indicating progressive phase formation. The reported permittivity values for the APO and PO phases are typically ~20–27 [2, 3] and ~26 [3], respectively, which are insufficient to explain the observed increase fully. This suggests the coexistence of the T-phase, known to exhibit a higher dielectric constant of ~40–47. [4-6] Notably, C310$_{PMA}$ exhibits a dielectric permittivity of ~45, closely matching that of the T-phase. Therefore, the observed FFE behavior is more appropriately attributed to T-phase-based field-induced ferroelectricity rather than AFE characteristics originating from the APO phase.

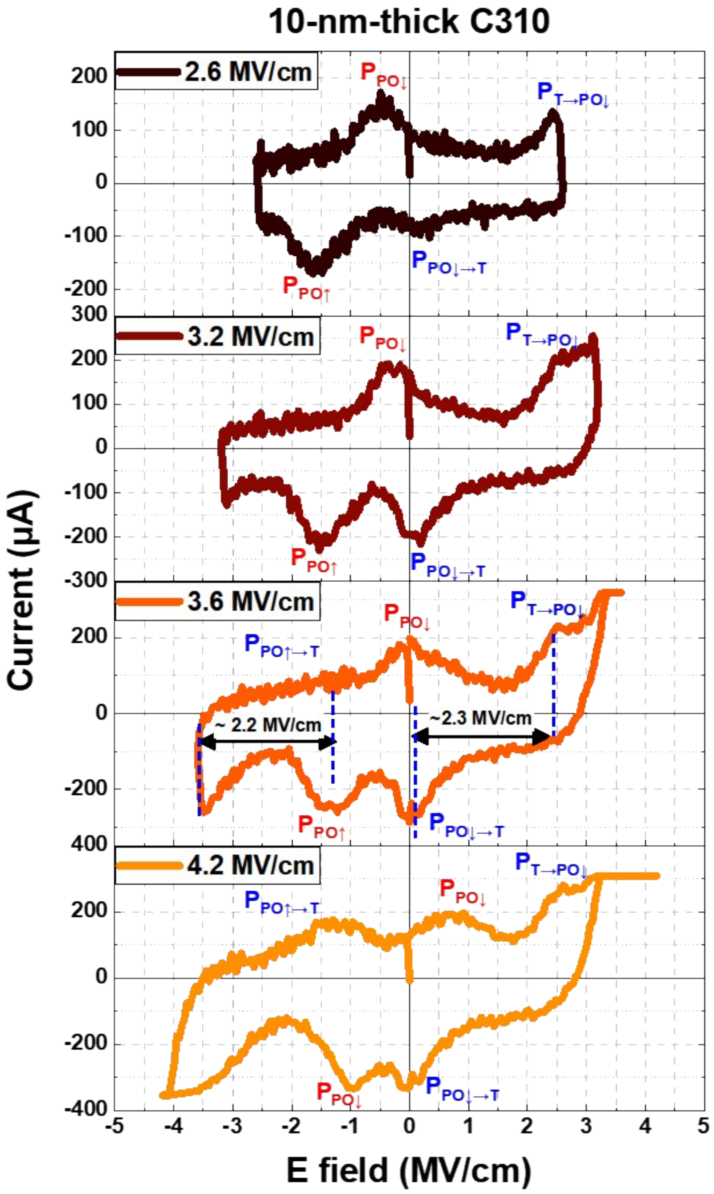

Figure S3. Pristine state I-E curves of 10-nm-thick C310 thin films with increasing measurement field. In the measurement field 3.6 MV/cm, the FFE forward switching value of the negative region, i.e., the peak value of $P_{T\rightarrow PO\uparrow}$, is indistinguishable due to the leakage current, but the reverse switching peak, i.e., $P_{PO\uparrow\rightarrow T}$, begins to appear. In the measurement field 4.2 MV/cm, the reverse switching peak of the FFE is evident in the negative field region.

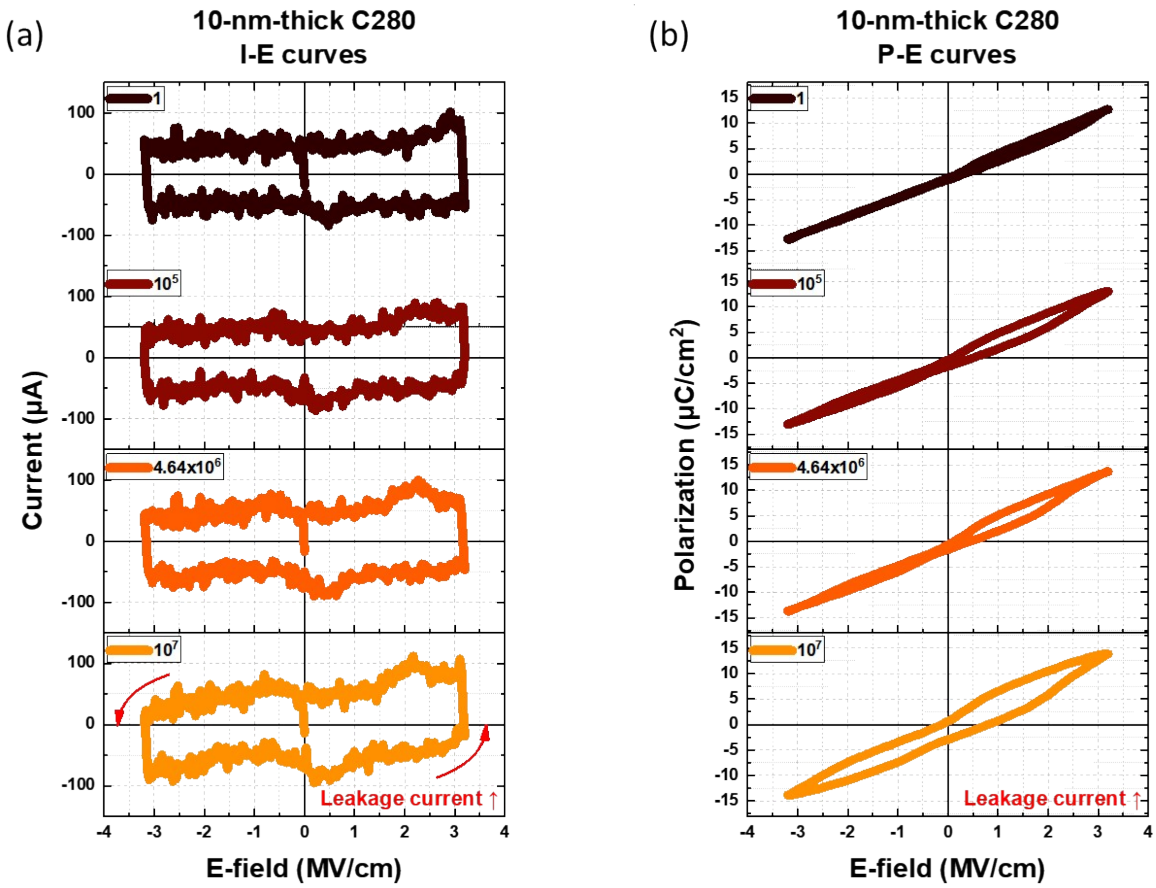

Figure S4. Evolution of (a) I–E and (b) P–E curves of the C280 film under field cycling at 3.2 MV/cm and 100 kHz. As shown, a noticeable increase in leakage current is observed after 10^7 cycles. This degradation behavior is likely attributed to the higher proportion of the amorphous phase in the C280 film, which introduces a greater density of defect sites that can facilitate leakage pathways and accelerate electrical breakdown during prolonged cycling.

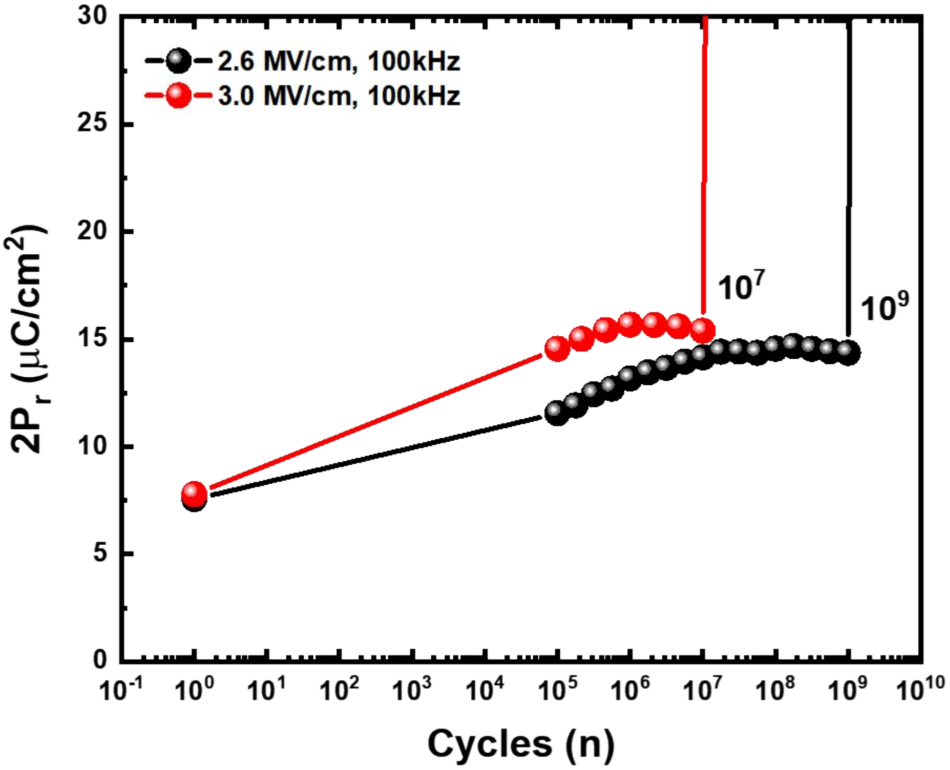

Figure S5. Results of the endurance test of the C310 film for the cycling field 2.6 MV/cm (black) and 3.0 MV/cm (red) at the frequency of 100 kHz.

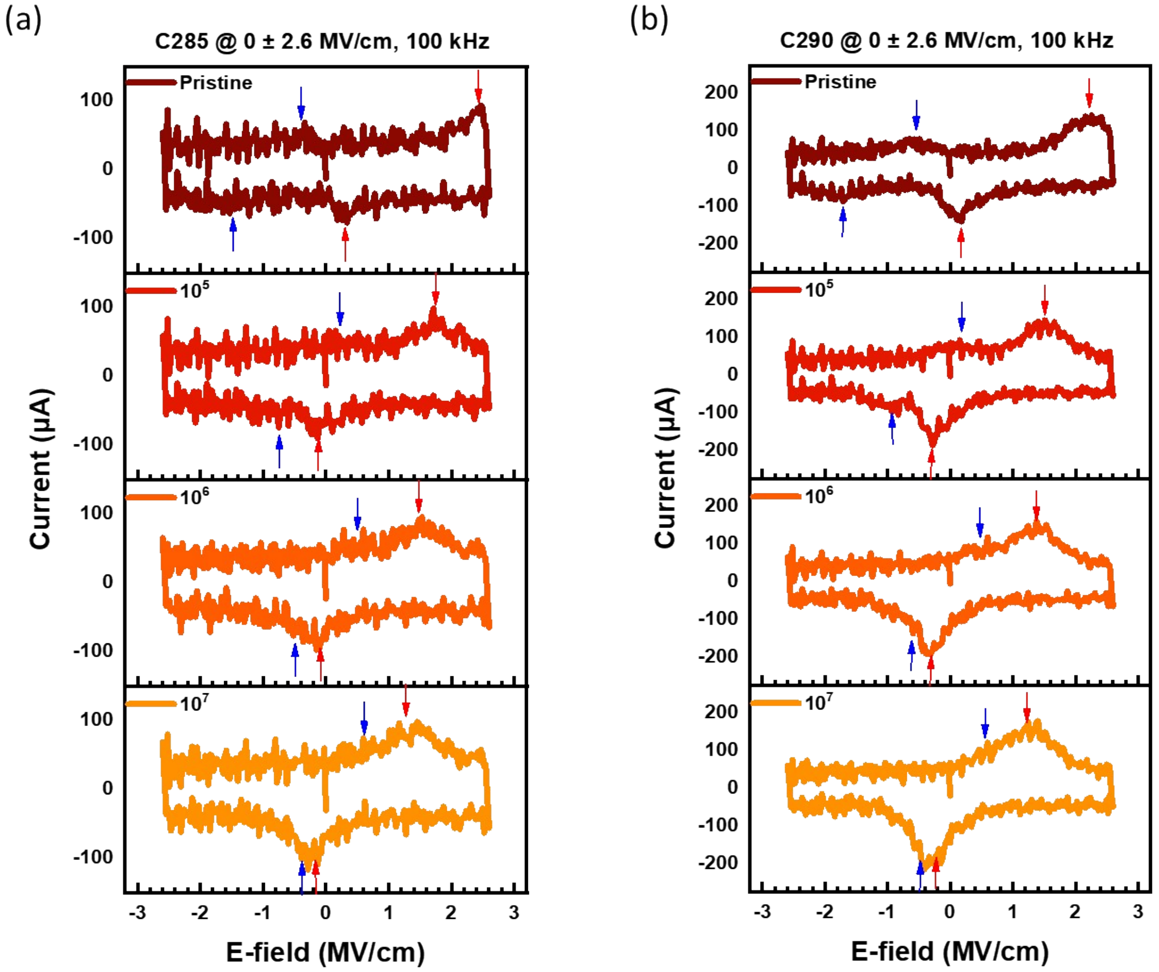

Figure S6. Evolution of I-E curves carried out on (a) C285 and (b) C290 film, respectively, by the field cycling at ± 2.6 MV/cm, 100 kHz without offset. The switching peaks from the FFE and FE regions are indicated by red and blue arrows, respectively.

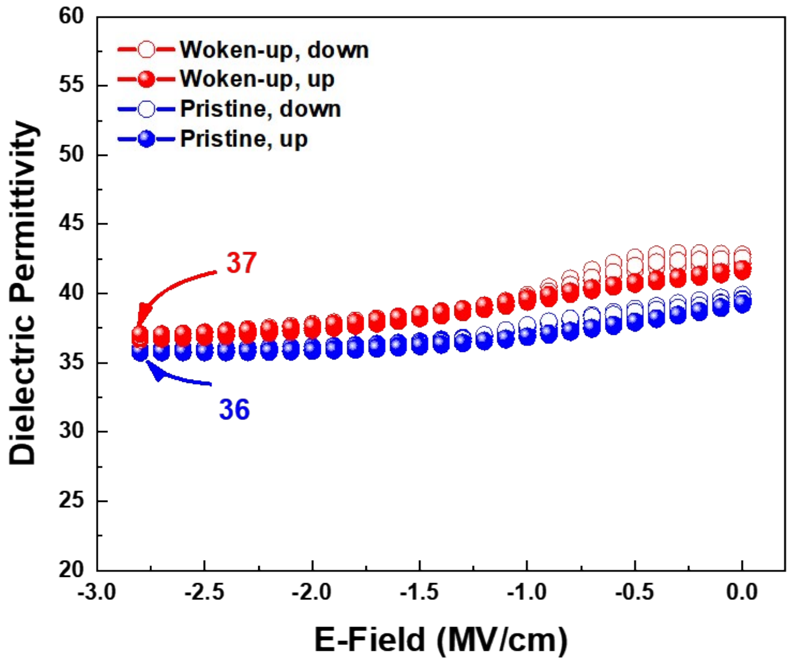

Figure S7. Dielectric permittivity at the pristine state and woken-up state of C310. The dielectric permittivity at -2.8 MV/cm, where the switching component is negligible, is about 36 in its pristine state and about 37 in its woken-up state (after field cycling at 2.6 MV/cm, 100 kHz), which is equivalent.

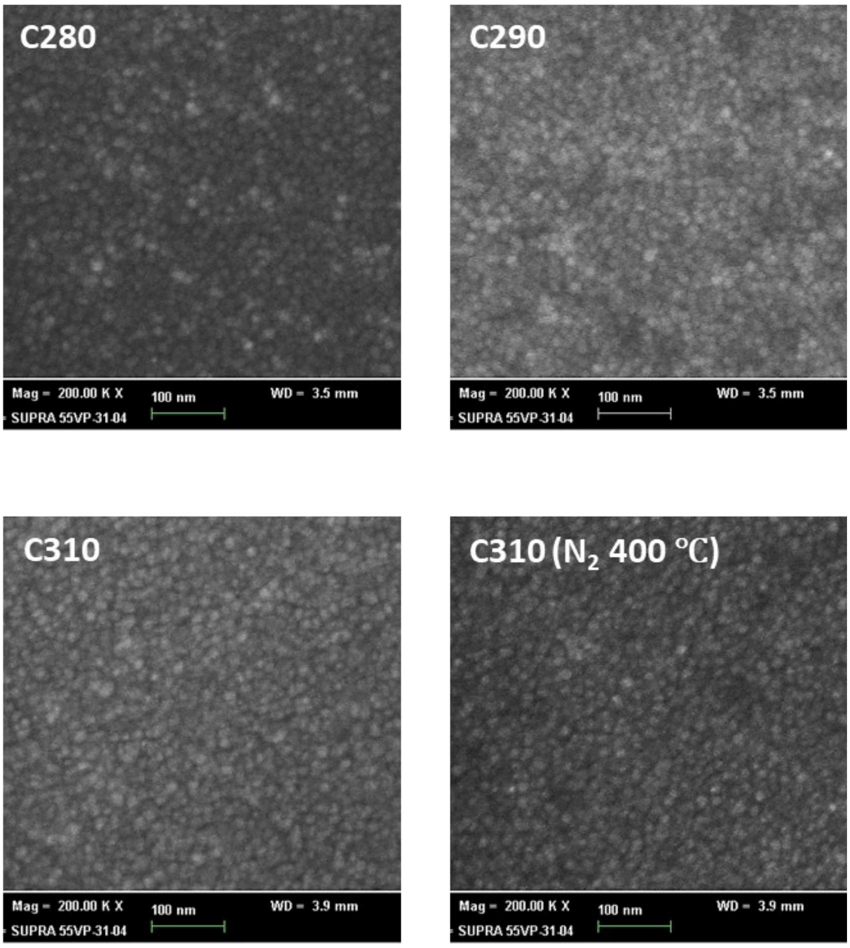

Figure S8. SEM plan-view images of 10-nm-thick C280, C290, C310, and annealed C310 thin films.

`

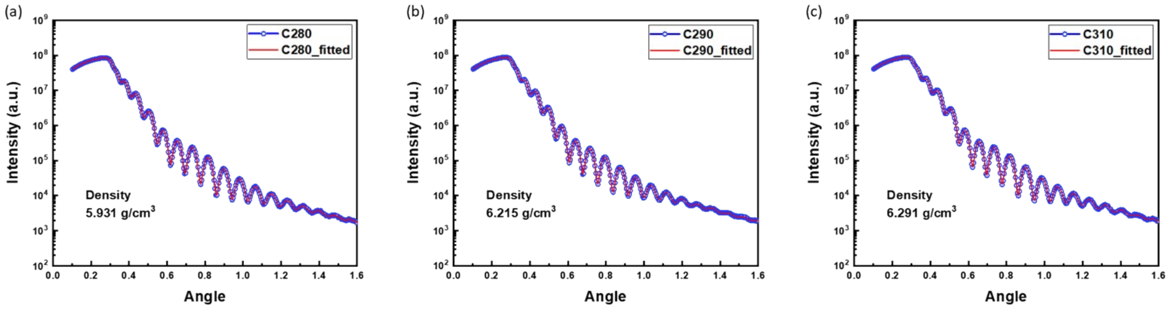

Figure S9. XRR results of 10-nm-thick C280, C290, and C310 on the 50-nm-thick TiN BE.

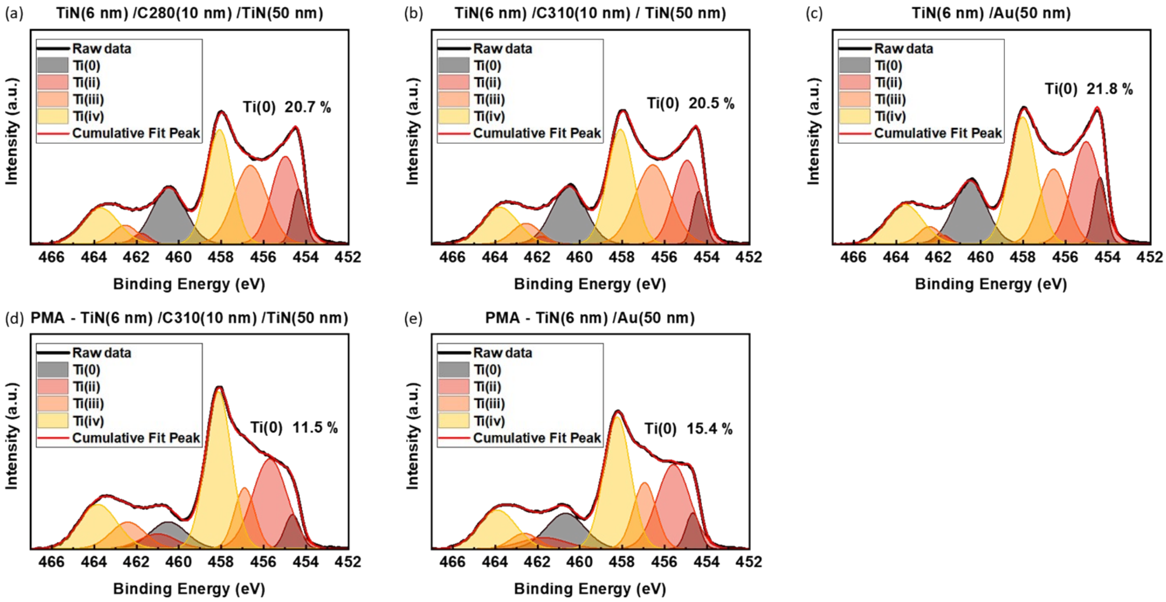

Figure S10. XPS deconvolution spectra: Ti 2p spectra of 6-nm-thick TiN TE deposited on (a) C280, (b) C310, and (c) Au films, respectively. Ti 2p spectra of PMA-treated 6-nm-thick TiN TE films deposited on (d) C310 and (e) Au, respectively. To compare the degree of oxidation of TiN TE for each condition, each figure displays the percentage of Ti(0), indicating the extent of Ti-N bonding.

References

1. X. Zhao, D. Ceresoli and D. Vanderbilt, *Physical Review B—Condensed Matter and Materials Physics*, 2005, **71**, 085107.
2. X. Zhao and D. Vanderbilt, *MRS Online Proceedings Library (OPL)*, 2002, **747**, T5. 2/N7. 2.
3. Y. Zhang, H.-X. Chen, L. Duan, J.-B. Fan, L. Ni and V. Ji, *Solid State Sciences*, 2018, **81**, 58-65.
4. X. Zhao and D. Vanderbilt, *Physical Review B*, 2002, **65**, 075105.
5. S. K. Kim and C. S. Hwang, *Electrochemical and Solid-State Letters*, 2007, **11**, G9.
6. J.-H. Kim, V. Ignatova, P. Kücher, J. Heitmann, L. Oberbeck and U. Schröder, *Thin Solid Films*, 2008, **516**, 8333-8336.